Deformations and Ruptures in Human Lenses With Cortical Cataract Subjected to Ex Vivo Simulated Accommodation

Ralph Michael,[1–3] Justin Christopher D'Antin,[1,2] Laura Pinilla Cortés,[1,2] Harvey John Burd,[4] Brian Sheil,[4] and Rafael I. Barraquer[1,2,5]

[1]Centro de Oftalmología Barraquer, Barcelona, Spain
[2]Institut Universitari Barraquer, Universitat Autònoma de Barcelona, Barcelona, Spain
[3]University Eye Clinic, Paracelsus Medical University, Salzburg, Austria
[4]Department of Engineering Science, University of Oxford, Oxford, United Kingdom
[5]Universitat Internacional de Catalunya, Barcelona, Spain

Correspondence: Rafael I. Barraquer, Centro de Oftalmología Barraquer, Carrer de Muntaner, 314, 08021 Barcelona, Spain; ralphm@barraquer.com.

Received: November 3, 2020
Accepted: December 16, 2020
Published: January 11, 2021

Citation: Michael R, D'Antin JC, Pinilla Cortés L, Burd HJ, Sheil B, Barraquer RI. Deformations and ruptures in human lenses with cortical cataract subjected to ex vivo simulated accommodation. *Invest Ophthalmol Vis Sci.* 2021;62(1):12. https://doi.org/10.1167/iovs.62.1.12

Purpose. Human cortical opacities are most commonly accompanied by changes in lens fiber structure in the equatorial region at the lens nucleus–cortex interface. Cortex and nucleus have different elastic properties, which change with age. We therefore subjected ex vivo lenses to simulated accommodation and studied the internal deformations to better understand the mechanism of cortical cataract formation.

Methods. Nine human donor lenses (33–88 years old) were tested using a bespoke radial stretching device for anterior eye segments. Seven of the lenses exhibited cortical cataracts. The other two lenses, without cataract, were used as controls. Frontal and cross-sectional images of the lens obtained during stretching facilitated measurements on equatorial lens diameter and central lens thickness in the stretched and unstretched states.

Results. Stretching caused the lens equatorial diameter to increase in all cases. Conversely, the lens central thickness showed no systematic variation during stretching. For four of the lenses with cortical cataract, ruptures were observed during stretching at the nucleus–cortex boundary adjacent to the cortical cataracts. Ruptures were not observed in the control lenses or in the three other lenses with cortical cataract.

Conclusions. Internal ruptures can occur in aged ex vivo lenses subjected to simulated disaccommodation. These ruptures occur at the nucleus–cortex interface; at this location, a significant stiffness discontinuity is expected to develop with age. It is hypothesized that ruptures occur in in vivo lenses during accommodation—or attempted accommodation.

Keywords: accommodation, presbyopia, cortical cataract

Cataracts are generally considered a multifactorial disease that is mainly caused by lifelong accumulation of oxidative stress, influenced by environmental and genetic factors, life style, exposure to ultraviolet radiation, diet, and systemic diseases.[1,2] Nuclear cataracts are generally believed to be caused by the accumulation of high-molecular-weight aggregates and increasing protein insolubility, resulting in lens opacity. Accumulation of fluorescent chromophores leads to a yellow to dark brunescent nuclear opacity.[3] For cortical cataracts, the repeated internal deformations that develop within the lens during accommodation may be a contributing causal factor, in addition to changes in the lens proteins.

The suggestion that accommodation forces might contribute to the formation of cortical cataract was first proposed by Wilhelm Schoen[4] in a lecture at Leipzig University in 1896. This hypothesis has been discussed, more recently, by Fisher[5] and later by Pau.[6] Angra et al.[7] suggested that shear stresses in the lens cortex could lead to a disturbed physiological milieu, allowing environmental factors such as ultraviolet radiation or other oxidative stress to alter the transparency in this area. Recently, we have shown that emmetropes and hyperopes (who are known to accommodate more than myopes) have a higher prevalence of cortical cataract than myopes.[8] The ex vivo simulated accommodation tests described in the current paper explore the potential link between cortical cataract and accommodation-induced internal lens deformations.

The morphology of cortical cataracts is characterized by an irregular fiber architecture and undulated, folded, and fractured groups of fiber cells at the border zone between the cortex and nucleus (Fig. 1).[9] These morphological observations indicate the presence of significant internal deformations within the lens. Previous finite element studies on simulated disaccommodation reported by Belaidi and Pierscionek[10] and Wang et al.[11] demonstrate that significant concentrations of stress appear to develop at locations in the lens where cortical cataracts typically occur.

Investigative Ophthalmology & Visual Science

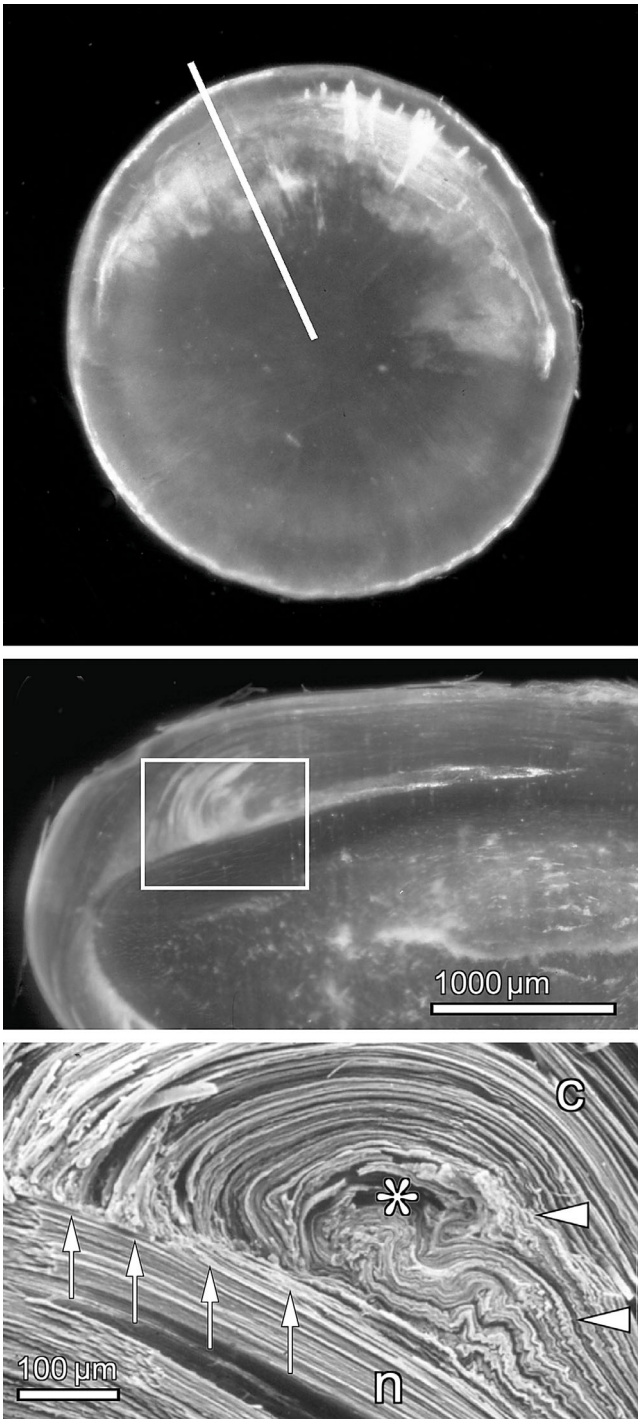

Figure 1. Human donor lens with cortical cataract. Frontal view (*top*) and cut at the axial plane (*center*), both imaged with dark-field illumination. Boxed area with groups of opaque fibers is shown below with scanning electron microscopy (*bottom*). Lens fibers at the border zone between the nuclear and cortical lens regions are broken (*arrows*), and the broken ends are directed against the nuclear fibers, which maintain a regular, uninterrupted organization. Further, note the curled (*asterisk*) and folded (*arrowheads*) fibers in the region adjoining the broken fibers. n, nuclear side; c, cortical side. Reprinted with permission from Michael R, Barraquer RI, Willekens B, van Marle J, Vrensen GFJM. Morphology of age-related cuneiform cortical cataracts: the case for mechanical stress. *Vision Res.* 2008;48(4):626–634. Copyright 2007 Elsevier Ltd.

Localized concentrations of stress could, initially, cause misalignment of intracellular lens protein, causing an increase in light scattering prior to gross lens fiber damage. Such an increase in light scattering at the border zone between the cortex and adult lens nucleus has been observed in Scheimpflug studies.[12] First occurrence of cortical cataracts has been documented from around 40 years of age onward in human donor lenses.[13]

Data on lens shear modulus determined from indentation tests[14,15] and spinning lens tests[16] indicate that in young lenses the nucleus is less stiff (i.e., has a lower value of shear modulus) than the cortex. The nucleus and cortex both increase in stiffness with age, but the stiffness of the nucleus increases at a faster rate than that of the cortex, with the consequence that, from middle age onward, the nucleus becomes increasingly stiffer than the cortex. These age-related stiffness changes mean that a sharp stiffness gradient develops at the nucleus–cortex boundary in later life. It is considered that repeated radial forces due to attempted accommodation will continue to be applied to the lens via the zonules, even beyond the age when the ability of the lens to accommodate has been lost. The stiffness gradient at the nucleus–cortex boundary seems likely to exacerbate the internal strains that develop in the equatorial cortex during attempted accommodation,[1,9,17,18] with consequential implications for the development of cortical cataract in late middle-aged and elderly subjects.

The current paper describes a set of ex vivo simulated disaccommodation tests on aged human lenses. The purpose of the tests is to explore potential correlations between the observed mechanical behavior of the lenses and the presence, or absence, of cortical cataract. A bespoke radial lens stretching device was used to conduct the tests.[19,20] Fisher[21] was probably the first to design a device for mounting anterior eye segments and imposing on them a prescribed radial stretch. Fisher's design imposed radial stretching via eight arms. Similar devices have been developed by Pierscionek,[22] Glasser and Campbell,[23] and Koopmans et al.[24] Enhanced forms of lens stretching apparatus incorporate the measurement of the external force applied to the sample.[25–28]

In interpreting the lens stretching tests, we consider the adult lens nucleus to be as defined in the morphological studies by Taylor et al.[29] Using this definition, the anterior and posterior cortex is approximately 650 µm thick and the equatorial cortex is approximately 750 µm. This cortex size corresponds to the location of a diffusion barrier found by Sweeney and Truscott[30] and peeling or hydrodissection experiments by Garland et al.[31] and Augusteyn.[32] There are alternative definitions of the dimensions of the lens cortex and nucleus, such as the Oxford Classification System, based on Scheimpflug images and which considers the lens at birth to be the lens nucleus.[33] In the Oxford Classification System, the anterior and posterior lens cortex is approximately 1200 µm thick, and the thickness of the equatorial cortex is approximately 2000 µm.

In lenses with cortical cataracts, a clear morphological distinction between lens cortex and adult nucleus is typically observed (Fig. 1). This border zone is usually found from 500 to 700 µm below the lens capsule.[9,34] Such a border zone has also been observed in in vivo studies using optical coherence tomography [35,36]

Investigative Ophthalmology & Visual Science

Table. Human Donor Lens Information and Descriptive Results of Lens Stretching

ID	Age (y)	Postmortem (h)	Nuclear Cataract Grade*	Cortical Cataract Circumference† (%)	Lens Diameter (mm)		Cortical Cataract Depth (mm)		Rupture Depth Unstretched (mm)	Rupture Circumference‡ (%)	Maximum Stretching Force (mN)
					Unstretched	Stretched	Unstretched	Stretched			
M71	33	45	0	—	9.30	9.71	—	—	—	—	75
M80	46	115	0	—	9.13	9.44	—	—	—	—	54
M82	78	107	4	100	9.64	9.76	0.590	0.640	—	—	53
M86	87	58	3	100	9.39	9.92	0.550	0.710	—	—	67
M85	74	73	5	31	9.83	10.28	0.550	0.730	—	—	69
M87	88	68	3	42	9.82	10.07	0.490	0.570	0.400	7	53
M83	85	97	4	39	9.74	10.08	0.710	0.810	0.690	10	68
M79	60	78	3	61	9.38	9.81	0.530	0.670	0.510	28	56
M69	86	40	3	44	9.97	10.38	0.540	0.710	0.480	44	75§
Mean	—	76	—	60	—	—	0.570	0.690	0.520	22	—

*Nuclear cataract grade according to BCN 10 scale (0–10).
† Cortical cataract along lens circumference as percentage of total lens equatorial perimeter.
‡Rupture along lens circumference as percentage of total lens equatorial perimeter.
§ The force for specimen M69 was estimated, because the ciliary body was not cut as in all other samples due to an oversight.

Methods

We studied the lenses of nine human donors provided by the Banco de Ojos para Tratamiento de la Ceguera (Barcelona, Spain), which included (1) seven lenses with cortical cataracts (between 60 and 88 years of age), and (2) two, relatively young control lenses (33 and 46 years of age) without cataracts (see Table). The donor eyes were stored at 8°C with a mean postmortem time of 76 hours (range, 40–115 hours). This research was conducted under the tenets of the Declaration of Helsinki and conformed to the Spanish regulations for the use of human tissues from organ donors.

Stretching tests of anterior segments of the donor eyes were conducted using a bespoke apparatus previously described in Pinilla et al.[19] and Michael et al.[20] The lenses were stretched using a stepper motor, and the resulting forces were measured using a 0.1-mN precision load cell from a commercial digital precision balance (Precisa BJ 210C; Precisa Gravimetrics AG, Dietikon, Switzerland). A digital camera (EOS 550D, 3456 × 2304 pixel resolution; Canon, Tokyo, Japan) mounted on a surgical microscope (Carl Zeiss Meditec AG, Jena, Germany) was used to take frontal images of the donor lens during stretching. Scheimpflug images of the lens cross-section were captured at each loading stage using the charge-coupled device sensor from a digital camera (NEX-5, 2448 × 1624 pixel resolution; Sony Corporation, Tokyo, Japan) and axial illumination from a Zeiss slit lamp. Each lens test was comprised of three or four measurement cycles, each involving 10 increments of stretching followed by 10 increments of relaxing (total of 2500 µm stretching distance per cycle).[20]

Frontal images from the second stretching cycle were used for subsequent analysis of the lens equatorial diameter; cross-sectional Scheimpflug images were taken during a third or fourth cycle to evaluate lens thickness changes. The frontal images were also used to describe the cortical cataract and to detect ruptures inside the lens during stretching, recording both their depth below the lens capsule and their extension along the lens perimeter. Nuclear cataract was graded on a scale of 0 to 10 according to the BCN 10 chart.[37]

The protocol adopted in the radial lens stretching tests[19] involves making radial cuts in the ciliary muscle during the sample preparation process. This ensures that the radial force applied to the lens can be determined directly from external measurements. Finite-element analyses described in Hermans et al.[38] indicate that the force required to stretch a 29-year lens in vivo from a fully accommodated to a disaccommodated state is in the region 42 to 55 mN (depending on assumptions on the material properties).[14,15] Burd and Wilde[39] also employed finite-element analysis and reported that a computed force of 49 mN was required to stretch a 45-year lens from a fully accommodated to a disaccommodated state. Moreover, ex vivo lens stretching data in Pinilla et al.[19] indicate that a radial force in the region of 50 mN is needed to stretch the lens from an accommodated to a disaccommodated state. Augusteyn et al.[26] found a median force of 80 mN to stretch human lenses ex vivo from an accommodated to a disaccommodated state; however, this force was obtained with an intact ciliary body. The data in Panilla et al.[19] suggest that, when the ciliary body is intact, the force actually transmitted to the lens is about 50% of the externally applied force. Thus, the 80 mN from Augusteyn et al.[26] is also broadly consistent with the 50 to 60 mN applied in the current tests.

The stretching protocol consists of applying increments of radial displacement (250 µm) to the loading hooks that connect with the ciliary body.[19] The applied radial force is measured at the end of each displacement increment; this system does not allow the application of preset values of radial force. The measured radial forces increased as the displacement increments were applied; maximum values of the force—corresponding to the end of increment 10—are listed in the Table. We selected the increment (8, 9, or 10) where the measured force was in the range of 50 to 60 mN (considered to be representative of physiological conditions) to allow the results to be compared at approximately the same value of radial force.

Analysis of stretching-induced changes to lens shape was undertaken for both the equatorial lens diameter (frontal images) and the lens central thickness (cross-sectional Scheimpflug images). The lens equator is not perfectly circular; it was generally found to deform somewhat asymmetrically during stretching. To obtain data on lens diameter change during stretching, therefore, the projected area within the lens equatorial perimeter in frontal images was determined using image processing software; an equivalent lens diameter for a perfect circle with the same area was used for the evaluation.

Results

The two control lenses (33 and 46 years) had unstretched equatorial diameters of 9.30 and 9.13 mm, respectively, and

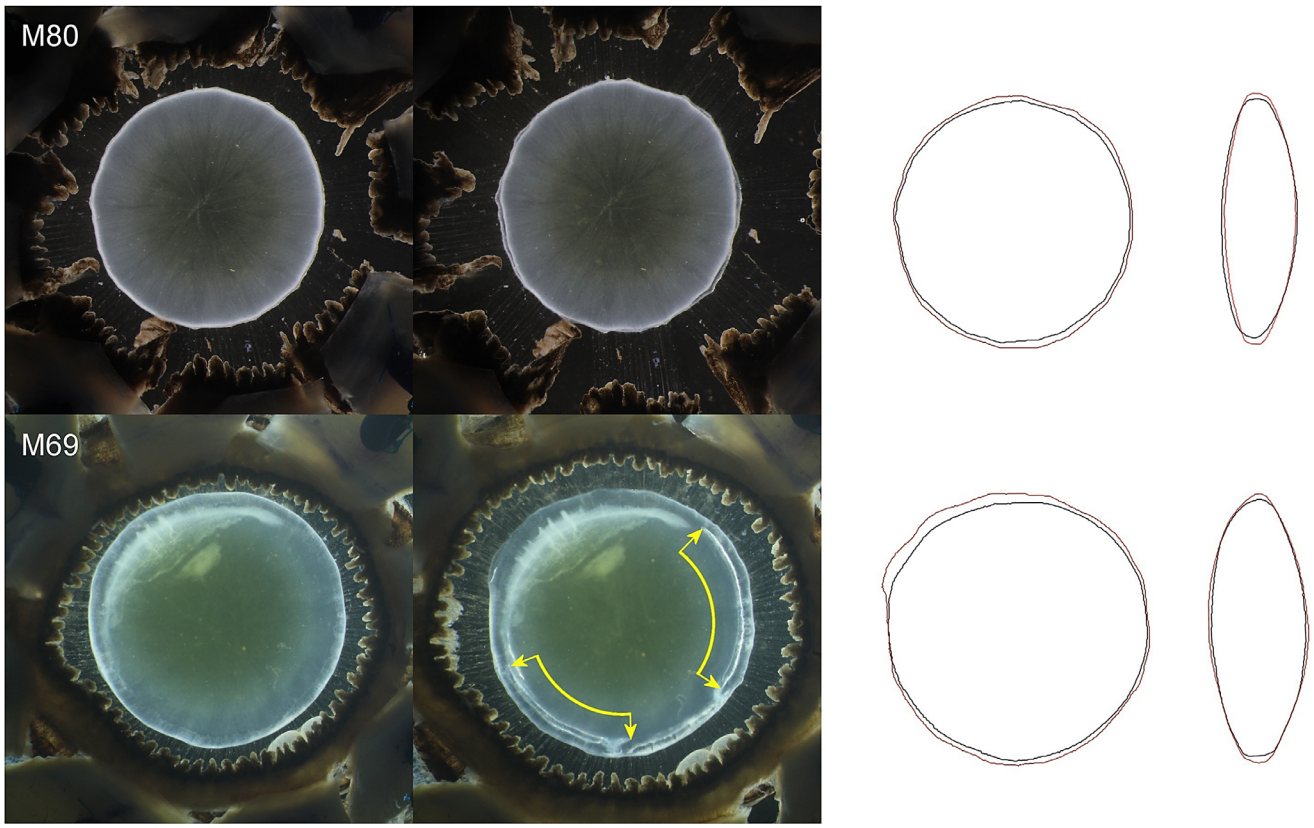

Figure 2. Two sample lenses, one control lens (*above*; M80, 46 years) and one with cortical cataract and internal ruptures after stretching (*below*; M69, 86 years). Frontal image on the left shows the first image, before the stretching experiments in the unstretched state. Frontal image on the right shows the last image after two or three cycles of stretching in the stretched state. The lens outline (*right*) is given for frontal view and cross-sectional view in the unstretched state (*black*) and with a stretching force of approximately 54 mN applied (*red*) during the same stretching cycle.

showed no indications of nuclear or cortical cataract. The unstretched equatorial diameter of the aged lenses (60 to 88 years) ranged between 9.4 and 10.0 mm. They showed nuclear cataract of between 3 and 5 on the BNC 10 scale, which is typical for this age range. The degree of cortical cataract was variable, occupying either the entire lens circumference or only part; on average, the cortical cataract was estimated to occupy about 60% of the lens circumference. Cortical cataracts were found on average at a depth of 570 µm below the lens capsule (Table).

Stretching-induced changes to lens shape were determined by comparing measurements taken at an average applied force of 54 mN (range, 50–60 mN). Both control lenses increased in equatorial diameter during stretching with a rather homogeneous extension around the lens equator (Fig. 2, Supplementary Fig. S1, Supplementary Videos S1 and S2). Because of the transparent media, no distinction between stretching of the cortex and nucleus could be observed. The lenses with cortical cataract also increased in equatorial diameter during stretching; however, some areas around the lens circumference stretched unsymmetrically, more in some areas and less in others. The cortex exhibited larger deformation near regions of observed opacifications compared to regions where the cortex was clear (Fig. 2, Supplementary Fig. S1). Four out of the seven cataractous lenses showed ruptures at the nucleus–cortex interface adjacent to the cortical cataracts (Supplementary Videos S3 and S4). These ruptures typically occurred at regions without cortical cataract; rupture occurred at 520 µm (on average) below the lens capsule. The ruptures extended on average 22% around the lens circumference, measured after four stretching cycles with a maximum force of 75 mN applied (see Table).

To allow for comparison, quantitative data on the stretched lens dimensions were determined at representative values of radial force in the range of 50 to 60 mN; these data are represented in Figure 3 as a percentage relative to the unstretched state. Total equatorial diameter increased in all lenses after stretching: by 2% to 6% in the aged lenses and by 3% to 4% in the control lenses. Total central thickness decreased in two aged lenses by 2%, remained unchanged (±1%) in another two aged lenses, and increased by 4% or 5% in a further two aged lenses. Total central thickness in the two control lenses decreased by 13% (M71) and 5% (M80). The equatorial diameter of the lens nucleus increased in both control lenses by 5% and remained practically unchanged (±1%) in the aged lenses. Consistent with the total central thickness changes, the central thickness of the nucleus in the control lenses decreased by 12% (M71) and 5% (M80) and remained practically unchanged (±1%) in the aged lenses (Fig. 3).

Discussion

This study was undertaken on human tissue from postmortem donors. Due to regulatory conditions and clinical

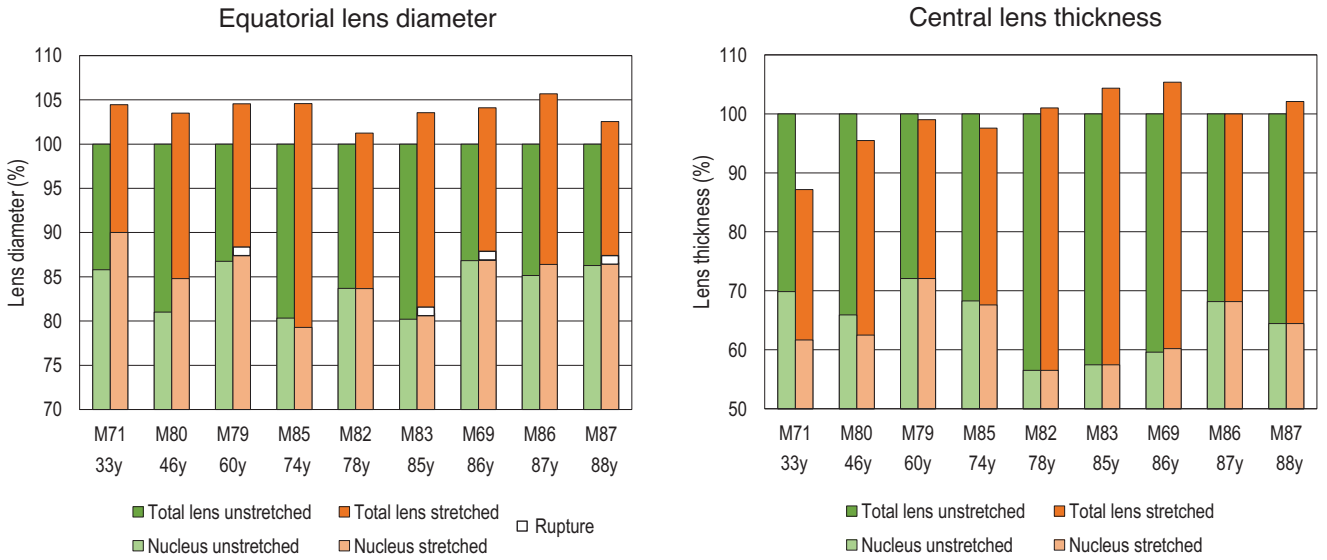

Figure 3. Equatorial lens diameter (*left*) and central lens thickness (*right*) for the total lens (*dark color*) and subdivided for the lens nucleus (*light color*) for the unstretched state (*green*) and stretched state (*orange*). Results are given as a percentage of the dimension with the total lens unstretched state set to 100%. Below are the specimen identification numbers (M71–M87) and the ages of the donor in years. Ruptures are indicated with a small *white rectangle*. Lenses are stretched with an average force of 54 mN (10^{-3} Newton). The radial force applied to the lens for specimen M69 was estimated, because the ciliary body was not cut as in all other samples due to an oversight.

schedules for corneal transplants, the time between death and our experiments varied between 40 and 115 hours (see Table). With longer postmortem times, the lens surface can become more opaque, and there is an increased risk of lens capsule detachment during stretching, as was observed in one sample (M80).

In most of the lenses, the equatorial lens diameter changed unsymmetrically around the lens circumference during stretching; therefore, we estimated the lens diameter by calculating the projected lens surface, in both the unstretched and fully stretched state and converted these surfaces to a circle with the same area. Determinations of the surface area were conducted using high-resolution images. The lens thickness was measured in Scheimpflug images. In lenses with pronounced cataract, the posterior lens capsule is difficult to visualize, so there is some uncertainty in the lens thickness data, particularly in the aged lenses.

On the basis of the procedures in Pinilla et al.,[19] the ciliary muscle was cut radially in the sample preparation protocol to ensure that all of the externally applied radial force was applied directly to the lens. Due to an oversight, the ciliary body in sample M69 was not radially cut. In this case, on the basis of data in Pinilla et al.,[19] we estimated the radial force applied to the lens as 50% of the measured force for the case where the ciliary body is intact.

Considering an aged human lens with standard dimensions according to Al-Ghoul et al.[40] (9.8-mm diameter and 4.87-mm thickness), the percentage changes in lens diameter due to stretching for the control lenses were 3% and 4% (0.30 and 0.40 mm, respectively). The percentage changes in lens thickness in the control lenses were 5% and 13% (0.24 and 0.63 mm, respectively). This is in good agreement with results from other groups. For example, in a large study from the United States and India, 40-year-old ex vivo human donor lenses, with intact ciliary bodies, were stretched at 100 mN (approximately equivalent to 50 mN in our samples with the ciliary body cut) and showed an average lens diameter change of 0.33 mm.[26] Another similar smaller study with human donor lenses (mean age 40 years) showed a lens diameter change of about 0.45 mm.[41] In vivo estimations with optical coherence tomography and magnetic resonance imaging in subjects about 40 years old and with 5 or 8 diopters accommodation stimulus resulted in a lens diameter change between 0.30 and 0.40 mm.[42,43]

Our data on lens deformations due to stretching in the aged lenses were somewhat surprising. Aged human donor lenses showed similar, or even greater, changes in lens diameter (2%–6%) than the control lenses (3%–4%) during stretching at the reference radial force of 54 mN. Lens thickness remained unchanged in five aged lenses but increased by 4% or 5% in two aged lenses during stretching.

These results demonstrate that the lens cortex remains deformable in aged lenses. The lens nucleus in aged lenses, however, appeared to remain undeformed during stretching; this is in contrast to the control lenses. These observations suggest that, consistent with prior data on lens shear modulus, the nucleus has a relatively high stiffness in aged lenses. Remarkably, the lens thickness increased in some of the aged lenses (Fig. 3). In Supplementary Video S4 (sample M69), compression of the cortex at the equator is apparent, and cortical lens material is pushed to the lens pole, resulting in an increase of lens thickness during stretching.

The morphology, severity, size, and extension along the lens circumference of a cortical cataract is highly variable.[3,9,34] However, a common feature is a transparent zone below the lens capsule slightly above the cortical cataract (Fig. 1). In our dataset, this depth ranged from 490 to 710 µm, below which the cortical cataract was located. These measured depths are in good agreement with the range 350 to 700 µm based on 29 cortical cataract samples previously documented in the literature.[9]

During our lens stretching tests, ruptures caused nonuniform deformations to occur around the lens circumference; ruptures did not occur in all lenses. The ruptures

were typically located adjacent to the cortical cataracts (Fig. 2, Supplementary Fig. S1). For example, the two lenses (samples M82 and M86) with cortical cataract present along the entire circumference did not exhibit any ruptures. It is possible that the cortical cataract may behave similarly to scar tissue, with higher connectivity in these areas leading to a reduced probability of rupture.

The incidence of a rupture in the lens cortex did not appear to be correlated with postmortem time (Table). Lenses with and without rupture both had a median postmortem time of 73 hours, and a non-parametric Mann–Whitney U test comparing both groups was not significant ($P = 0.624$). We also investigated whether or not there was an effect of postmortem time on lens shape changes during stretching (Fig. 3). Spearman's rank correlation test indicated that lens diameter and thickness changes did not correlate with postmortem time; the coefficient ρ was –0.460 ($P = 0.213$) considering diameter and –0.167 ($P = 0.668$) considering thickness.

In all cases, ruptures occurred at a depth that was shallower than the cortical cataracts. One lens (M79) exhibited minor initial capsule damage at the 1 o'clock position (Supplementary Fig. S1). This minor damage may allow liquid to enter the lens and fill the cavity opened by the rupture, thereby allowing the rupture to propagate.

Conclusions

Observations made in radial lens stretching tests with physiological forces indicate that, although the nucleus does not deform, the cortex seems to retain some elasticity and can reshape itself somewhat around the nucleus. Internal ruptures can occur in aged lenses when subjected to simulated disaccommodation. These ruptures occur at the nucleus–cortex interface, where significant stiffness discontinuities are thought to develop with age. These observations suggest that the nucleus–cortex interface is vulnerable to mechanical deformation during accommodation, or attempted accommodation, with potential consequences for cataract formation. Therefore, mechanical strain in the lens induced by accommodation or disaccommodation may contribute to the formation of cortical cataract; however, the current experiments cannot establish a causal link between rupture and cortical cataract.

Acknowledgments

Disclosure: **R. Michael,** None; **J.C. D'Antin,** None; **L. Pinilla Cortés,** None; **H.J. Burd,** None; **B. Sheil,** None; **R.I. Barraquer,** None

References

1. Vrensen GF. Early cortical lens opacities: a short overview. *Acta Ophthalmol*. 2009;87(6):602–610.
2. Michael R. Development and repair of cataract induced by ultraviolet radiation. *Ophthalmic Res*. 2000;32(Suppl 1):ii–iii; 1–44.
3. Michael R, Bron AJ. The ageing lens and cataract: a model of normal and pathological ageing. *Philos Trans R Soc Lond B Biol Sci*. 2011;366(1568):1278–1292.
4. Schoen W. *Die geschichtliche Entwicklung unserer Kenntnis der Staarkrankheit – Antritts-Vorlesung am 26. Oktober 1896 – Universität Leipzig*. Leipzig: Verlag von Alfred Langkammer; 1897:1–26.
5. Fisher RF. Human lens fibre transparency and mechanical stress. *Exp Eye Res*. 1973;16(1):41–49.
6. Pau H. Cortical and subcapsular cataracts: significance of physical forces. *Ophthalmologica*. 2006;220(1):1–5.
7. Angra SK, Adhikari KP, Dada VK. Refractive error stress in the aetiology of senile cataract. *Indian J Ophthalmol*. 1986;34(1):1–5.
8. Michael R, Pareja-Arico L, Rauscher FG, Barraquer RI. Cortical cataract and refractive error. *Ophthalmic Res*. 2019;62(3):157–165.
9. Michael R, Barraquer RI, Willekens B, van Marle J, Vrensen GF. Morphology of age-related cuneiform cortical cataracts: the case for mechanical stress. *Vision Res*. 2008;48(4):626–634.
10. Belaidi A, Pierscionek BK. Modeling internal stress distributions in the human lens: can opponent theories coexist? *J Vis*. 2007;7(11):1–12.
11. Wang K, Venetsanos D, Wang J, Pierscionek BK. Gradient moduli lens models: how material properties and application of forces can affect deformation and distributions of stress. *Sci Rep*. 2016;6:31171.
12. Fujisawa K, Sasaki K. Changes in light scattering intensity of the transparent lenses of subjects selected from population-based surveys depending on age: analysis through Scheimpflug images. *Ophthalmic Res*. 1995;27(2):89–101.
13. Vrensen G, Willekens B. Classification and prevalence of early senile lens opacities in human donor eyes. *Dev Ophthalmol*. 1989;17:181–187.
14. Weeber HA, Eckert G, Pechhold W, van der Heijde RG. Stiffness gradient in the crystalline lens. *Graefes Arch Clin Exp Ophthalmol*. 2007;245(9):1357–1366.
15. Heys KR, Cram SL, Truscott RJ. Massive increase in the stiffness of the human lens nucleus with age: the basis for presbyopia? *Mol Vis*. 2004;10:956–963.
16. Wilde GS, Burd HJ, Judge SJ. Shear modulus data for the human lens determined from a spinning lens test. *Exp Eye Res*. 2012;97(1):36–48.
17. Fisher RF. Senile cataract. A comparative study between lens fibre stress and cuneiform opacity formation. *Trans Ophthalmol Soc UK*. 1970;90:93–109.
18. Beebe DC. The physiology and pathobiology of the lens. In: McManus LM, Mitchell RN , eds. *Pathobiology of Human Disease*. Cambridge, MA: Academic Press; 2014:2072–2083.
19. Pinilla CL, Burd HJ, Montenegro GA, et al. Experimental protocols for ex vivo lens stretching tests to investigate the biomechanics of the human accommodation apparatus. *Invest Ophthalmol Vis Sci*. 2015;56(5):2926–2932.
20. Michael R, Mikielewicz M, Gordillo C, Montenegro GA, Pinilla CL, Barraquer RI. Elastic properties of human lens zonules as a function of age in presbyopes. *Invest Ophthalmol Vis Sci*. 2012;53(10):6109–6114.
21. Fisher RF. The force of contraction of the human ciliary muscle during accommodation. *J Physiol (Lond)*. 1977;270(1):51–74.
22. Pierscionek BK. In vitro alteration of human lens curvatures by radial stretching. *Exp Eye Res*. 1993;57(5):629–635.
23. Glasser A, Campbell MC. Presbyopia and the optical changes in the human crystalline lens with age. *Vision Res*. 1998;38(2):209–229.
24. Koopmans SA, Terwee T, Barkhof J, Haitjema HJ, Kooijman AC. Polymer refilling of presbyopic human lenses in vitro restores the ability to undergo accommodative changes. *Invest Ophthalmol Vis Sci*. 2003;44(1):250–257.
25. Manns F, Parel JM, Denham D, et al. Optomechanical response of human and monkey lenses in a lens stretcher. *Invest Ophthalmol Vis Sci*. 2007;48(7):3260–3268.
26. Augusteyn RC, Mohamed A, Nankivil D, et al. Age-dependence of the optomechanical responses of ex vivo human lenses from India and the USA, and the force

required to produce these in a lens stretcher: the similarity to in vivo disaccommodation. *Vision Res*. 2011;51(14):1667–1678.
27. Ehrmann K, Ho A, Parel JM. Biomechanical analysis of the accommodative apparatus in primates. *Clin Exp Optom*. 2008;91(3):302–312.
28. Reilly MA, Hamilton PD, Perry G, Ravi N. Comparison of the behavior of natural and refilled porcine lenses in a robotic lens stretcher. *Exp Eye Res*. 2009;88(3):483–494.
29. Taylor VL, Al-Ghoul KJ, Lane CW, Davis VA, Kuszak JR, Costello MJ. Morphology of the normal human lens. *Invest Ophthalmol Vis Sci*. 1996;37(7):1396–1410.
30. Sweeney MH, Truscott RJ. An impediment to glutathione diffusion in older normal human lenses: a possible precondition for nuclear cataract. *Exp Eye Res*. 1998;67(5):587–595.
31. Garland DL, Duglas-Tabor Y, Jimenez-Asensio J, Datiles MB, Magno B. The nucleus of the human lens: demonstration of a highly characteristic protein pattern by two-dimensional electrophoresis and introduction of a new method of lens dissection. *Exp Eye Res*. 1996;62(3):285–291.
32. Augusteyn RC. On the growth and internal structure of the human lens. *Exp Eye Res*. 2010;90(6):643–654.
33. Sparrow JM, Bron AJ, Brown NA, Ayliffe W, Hill AR. The Oxford Clinical Cataract Classification and Grading System. *Int Ophthalmol*. 1986;9(4):207–225.
34. Vrensen GF, Otto C, Lenferink A, et al. Protein profiles in cortical and nuclear regions of aged human donor lenses: a confocal Raman microspectroscopic and imaging study. *Exp Eye Res*. 2016;145:100–109.
35. Uhlhorn SR, Borja D, Manns F, Parel JM. Refractive index measurement of the isolated crystalline lens using optical coherence tomography. *Vision Res*. 2008;48(27):2732–2738.
36. de Castro A, Benito A, Manzanera S, et al. Three-dimensional cataract crystalline lens imaging with swept-source optical coherence tomography. *Invest Ophthalmol Vis Sci*. 2018;59(2):897–903.
37. Barraquer RI, Pinilla CL, Allende MJ, et al. Validation of the nuclear cataract grading system BCN 10. *Ophthalmic Res*. 2017;57(4):247–251.
38. Hermans EA, Dubbelman M, van der Heijde GL, Heethaar RM. Change in the accommodative force on the lens of the human eye with age. *Vision Res*. 2008;48(1):119–126.
39. Burd HJ, Wilde GS. Finite element modelling of radial lentotomy cuts to improve the accommodation performance of the human lens. *Graefes Arch Clin Exp Ophthalmol*. 2016;254(4):727–737.
40. Al-Ghoul KJ, Nordgren RK, Kuszak AJ, Freel CD, Costello MJ, Kuszak JR. Structural evidence of human nuclear fiber compaction as a function of ageing and cataractogenesis. *Exp Eye Res*. 2001;72(3):199–214.
41. Ziebarth NM, Borja D, Arrieta E, et al. Role of the lens capsule on the mechanical accommodative response in a lens stretcher. *Invest Ophthalmol Vis Sci*. 2008;49(10):4490–4496.
42. Richdale K, Sinnott LT, Bullimore MA, et al. Quantification of age-related and per diopter accommodative changes of the lens and ciliary muscle in the emmetropic human eye. *Invest Ophthalmol Vis Sci*. 2013;54(2):1095–1105.
43. Strenk SA, Semmlow JL, Strenk LM, Munoz P, Gronlund-Jacob J, DeMarco JK. Age-related changes in human ciliary muscle and lens: a magnetic resonance imaging study. *Invest Ophthalmol Vis Sci*. 1999;40(6):1162–1169.

Supplementary Material

Supplementary Video S1. Lens M80 in frontal view, first stretching cycle.

Supplementary Video S2. Lens M80 in cross-sectional view, first stretching cycle.

Supplementary Video S3. Lens M69 in frontal view, first, second and third stretching cycle.

Supplementary Video S4. Lens M69 in cross-sectional view, first stretching cycle.

Investigative Ophthalmology & Visual Science